Title

LB791 Endoplasmic reticulum calcium regulates epidermal barrier response and desmosomal structure

Permalink

https://escholarship.org/uc/item/2qg232xv

Journal

Journal of Investigative Dermatology, 136(8)

ISSN

0022-202X

Authors

Celli, A
Crumrine, DA
Meyer, J
et al.

Publication Date

2016-08-01

DOI

10.1016/j.jid.2016.05.042

Peer reviewed

Endoplasmic Reticulum Calcium Regulates Epidermal Barrier Response and Desmosomal Structure

Anna Celli[1], Debra Crumrine[1], Jason M. Meyer[1] and Theodora M. Mauro[1]

Ca^{2+} fluxes direct keratinocyte differentiation, cell-to-cell adhesion, migration, and epidermal barrier homeostasis. We previously showed that intracellular Ca^{2+} stores constitute a major portion of the calcium gradient especially in the stratum granulosum. Loss of the calcium gradient triggers epidermal barrier homeostatic responses. In this report, using unfixed ex vivo epidermis and human epidermal equivalents we show that endoplasmic reticulum (ER) Ca^{2+} is released in response to barrier perturbation, and that this release constitutes the major shift in epidermal Ca^{2+} seen after barrier perturbation. We find that ER Ca^{2+} release correlates with a transient increase in extracellular Ca^{2+}. Lastly, we show that ER calcium release resulting from barrier perturbation triggers transient desmosomal remodeling, seen as an increase in extracellular space and a loss of the desmosomal intercellular midline. Topical application of thapsigargin, which inhibits the ER Ca^{2+} ATPase activity without compromising barrier integrity, also leads to desmosomal remodeling and loss of the midline structure. These experiments establish the ER Ca^{2+} store as a master regulator of the Ca^{2+} gradient response to epidermal barrier perturbation, and suggest that ER Ca^{2+} homeostasis also modulates normal desmosomal reorganization, both at rest and after acute barrier perturbation.

INTRODUCTION

A competent epidermal barrier is required for terrestrial survival. A variety of components such as secreted and processed lipid, adherens or tight junctions, and desmosomes contribute to epidermal barriers to water loss, shear forces, and external toxins or microbes. These components must reorganize in response to both normal epidermal differentiation and epidermal perturbation such as barrier disruption or wounding. Ca^{2+} controls several of the processes that keep the epidermis in equilibrium. The epidermal Ca^{2+} gradient controls barrier recovery by stimulating lipid release after barrier perturbation. Ca^{2+} fluxes also control keratinocyte migration during wound healing (Trollinger et al., 2002). On the cellular level, Ca^{2+} controls desmosome formation and remodeling, via endoplasmic reticulum (ER) Ca^{2+} release and protein kinase C-alpha activation (Hobbs et al., 2011; Thomason et al., 2012; Wallis et al., 2000). Desmosome formation requires Ca^{2+}. However, contrary to other cell-to-cell junctions such as adherens junctions, fully formed desmosomes adopt a stronger, calcium-independent hyperadhesive state, which is characterized functionally by resistance to disruption by EGTA calcium chelation, and morphologically by the presence of a dense intercellular midline at the electron microscopy level (Garrod et al., 2005). Desmosomes in the hyperadhesive state retain plasticity (Tariq et al., 2015) and have been shown to respond to wounding by reverting to a non-hyperadhesive, calcium-dependent state through a protein kinase C-alpha-dependent process (Garrod et al., 2005) to allow cell migration and re-epithelialization of the wound. Hobbs et al. (2011) demonstrated that ER calcium release causes changes in desmosomal assembly and intercellular adhesive strength of fully formed desmosomes in cultured human keratinocytes.

Although Ca^{2+} fluxes regulate crucial processes in epidermal differentiation and barrier homeostasis (Baek et al., 2013; Elias et al., 2002a, 2002b; Yuspa et al., 1989), the signaling pathways by which the Ca^{2+} gradient responds to barrier perturbation is not well understood. In normal human and murine epidermis, Ca^{2+} levels are low in the basal layer, increase to a maximum in the stratum granulosum (SG), and drop to a minimum in the stratum corneum (SC) (Menon and Elias, 1991; Menon et al., 1992). This Ca^{2+} gradient depends on a competent epidermal barrier (Mauro et al., 1998; Menon and Elias, 1991; Menon et al., 1994), which in turn is formed by keratinocyte Ca^{2+} uptake, release, and influx (Feingold and Denda, 2012; Hu et al., 2000; Man et al., 1997). Studies from our group (Celli et al., 2010) and others (Adams et al., 2012; Cornelissen et al., 2007; Denda et al., 2012) have identified intracellular, rather than extracellular, calcium stores as the main components of the epidermal calcium gradient, and shown that ER Ca^{2+} release alone can control barrier repair processes (Celli et al., 2011).

[1]Dermatology Service, Department of Veterans Affairs Medical Center, and Department of Dermatology, University of California, San Francisco, California, USA

Correspondence: Anna Celli, VAMC/UCSF Dermatology Research, 1700 Owens Street, 3rd Floor, San Francisco, California 94158-0002, USA. E-mail: Anna.celli2@ucsf.edu

Although we previously have shown that the Ca^{2+} gradient in unperturbed epidermis largely is formed by organelle (i.e., ER) stores (Celli et al., 2010), how ER Ca^{2+} responds to barrier perturbation to shape changes in the Ca^{2+} gradient has not yet been defined. In this report, we show that ER Ca^{2+} is released in response to barrier perturbation, resulting in a transient increase in tissue $[Ca^{2+}]$, followed by later depletion. The time course of this transient increase has not been detected or defined by previous studies. Further, we find that barrier perturbation causes widening of the intercellular spaces and desmosome remodeling in the SG and stratum spinosum (SS), similar to that seen in tissue wounding (Garrod et al., 2005), likely allowing Ca^{2+} to freely diffuse out of the epidermis, and allowing transitional cells to move upward in the epidermis during barrier repair. Pharmacologic ER Ca^{2+} release with topical thapsigargin (TG) reproduces desmosome remodeling, even though the epidermal barrier is not perturbed. These data demonstrate that regulated ER Ca^{2+} release controls the epidermal Ca^{2+} gradient and desmosomal reorganization after barrier perturbation.

RESULTS

Calcium levels are transiently elevated after barrier perturbation in human skin

We first used human skin explants stained with calcium green 5N to monitor total free calcium fluxes after barrier perturbation using the fluorescence lifetime imaging (FLIM) technique previously described in Celli et al. (2010). This technique allowed us to image the full depth of the unsectioned tissue within the first 10 minutes after barrier abrogation. To control for changes due to simple mechanical stress with tape stripping, we also perturbed the barrier by acetone lipid extraction. Morphology of control and perturbed epidermal strata and false color images representing their respective calcium concentrations as measured by phasor-FLIM analysis are shown in Supplementary Figure S1 online. Because the epidermal calcium concentration exceeds the sensitivity of our method, a mean calcium concentration value cannot be calculated from our images. Therefore, to quantify and compare calcium levels from separate experiments, we calculated calcium concentration distribution histograms per each image and the calcium concentration corresponding to the peak of the distribution. Figure 1a and b represent the averaged position of the calcium concentration peaks in each epidermal layer. We observed a dramatic shift of the calcium concentration distribution toward higher calcium levels immediately after barrier perturbation in all epidermal layers (Figure 1a and b, respectively, and Supplementary Figure S1) in agreement with data previously reported in mice (Behne et al., 2011). To monitor calcium fluxes during barrier recovery, we imaged tape-stripped and acetone-treated samples 4 and 24 hours after perturbation. Four hours after perturbation, calcium levels were lower than baseline in all viable layers of tape-stripped samples in agreement with previous reports (Man et al., 1997; Menon et al., 1994), and in the SG of acetone-treated samples. Elevated calcium levels in the SS and stratum basale of acetone-treated samples (Figure 1b and Supplementary Figure S1) persist 4 hours after perturbation, likely as a consequence of persistent acetone exposure.

Within 10−24 hours after barrier perturbation, calcium levels in the viable epidermal layers returned to baseline values, whereas calcium levels in the SC of the acetone-treated samples remained slightly elevated. Localization of epidermal calcium pools before and after perturbation is shown in Supplementary Figure S1.

Morphological analysis of FLIM images showed that immediately after barrier perturbation, calcium levels are elevated both intracellularly and extracellularly in the viable epidermis (Figure 2a and Supplementary Figure S1). Moreover, we noticed that, although extracellular domains are well below the optical resolution of the microscope in the granular layer of intact epidermis, they become apparent immediately after barrier perturbation (Figure 2a) and display total calcium levels that are higher than in unperturbed skin, suggesting large calcium fluxes through the extracellular space. Analysis of low-magnification ($\times 4,800$) micrographs revealed extended wider gaps between cells in the SG and SS after barrier perturbation by either tape stripping or acetone (Figure 2b). Interestingly, whereas extracellular spaces present wider gaps after barrier perturbation, desmosomes maintain a tightly closed conformation as shown in Figure 3c and discussed below. We used $\times 4,800$ and $\times 10,000$ electron microscopy micrographs to semiquantify changes in cell-to-cell distances, and found that barrier perturbation results in statistically significant widening of intercellular spaces (Table 1).

ER calcium is released after barrier perturbation

To test the hypothesis that increased intracellular calcium was due to release from intracellular stores, we used fully differentiated human epidermal equivalents (HEEs), which can be transfected with organelle-targeted calcium indicators. Our HEEs display a calcium concentration profile as measured by FLIM (Figure 3a and Sun et al., 2015) and ion-capture cytochemistry (Petrova et al., 2014), and barrier recovery after tape stripping (Sun et al., 2015) similar to that of human and murine epidermis.

We then transfected HEEs with the cameleon-based ER targeted calcium sensor D1ER (Palmer et al., 2006) to monitor the ER calcium profile at baseline and after perturbation. In the presence of calcium, Förster resonance energy transfer (FRET) between the cyan fluorescent protein (CFP) and yellow fluorescent protein (YFP) moieties of D1ER occurs, and the ratio between the YFP and CFP intensities ($R = I_{(YFP)}/I_{(CFP)}$) increases. In fully differentiated and unperturbed HEEs, the ratio (R) was significantly higher in the SG cells than in the SS and stratum basale cells, indicating higher calcium sequestration in the ER in the upper epidermal layers (Figure 3b). Because ER calcium release leads to lipid secretion and physiological apoptosis in SG keratinocytes (Celli et al., 2012), we specifically monitored the ER calcium levels in SG cells in perturbed and unperturbed HEEs over a course of 40 minutes (Figure 3c). Although unperturbed HEEs displayed constant ER calcium levels in the SG over this time interval, we observed a 20% decrease in the FRET ratio in the SG immediately after tape stripping, demonstrating that calcium is, in fact, released from the ER into the cytosol of granular cells after barrier perturbation. The average FRET ratio then increased until plateauing above the baseline, indicating active store refill. In a separate experiment, we
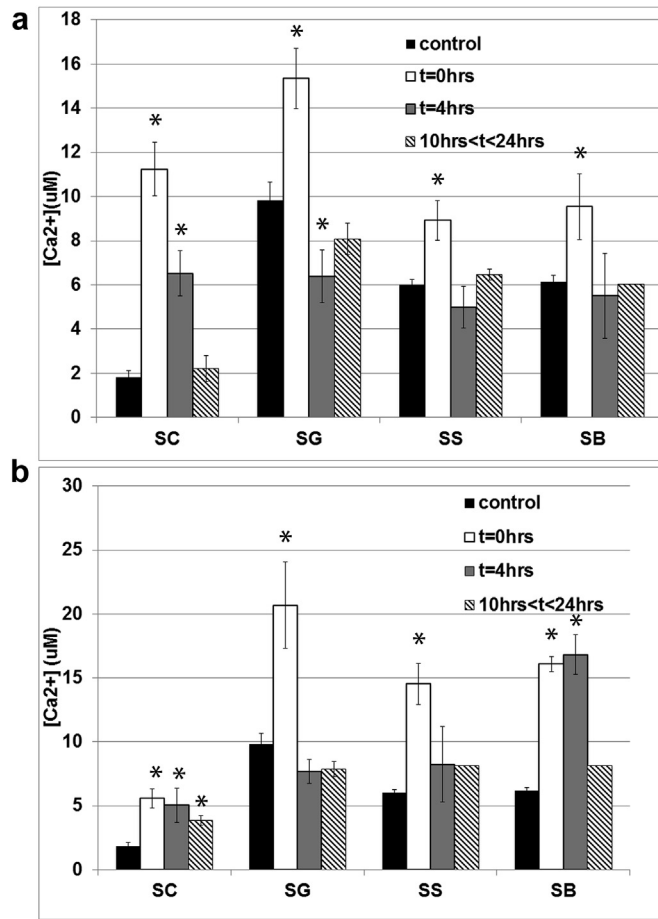
Figure 1. FLIM-based detection of calcium fluxes in human epidermis after barrier perturbation. (a) Calcium concentration distribution peak values in different epidermal strata at $t = 0$, 4, and >10 hours after barrier perturbation by tape stripping. Samples imaged between 10 and 24 hours after perturbation show no difference in morphology or $[Ca^{+2}]$ and are therefore grouped in the same time interval. (b) Calcium concentration distribution peak values in different epidermal strata at $t = 0$, 4, and >10 hours after barrier perturbation by acetone lipid extraction. Data are presented as mean $\pm$ SEM; $n = 2-4$ samples per time point/condition and $1-4$ optical sections per epidermal strata. Double-tailed t-tests between unperturbed control calcium levels (black bars) and tape-stripped (a) and acetone (b) calcium levels at different time points (horizontal striped bars: $t = 0$; gray bars: $t = 4$ hours; diagonal striped bars: $t = 24$ hours) were performed. Asterisks represent statistically significant deviations of calcium levels at different times after perturbation from the unperturbed calcium levels $P < 0.02$. FLIM, fluorescence lifetime imaging; SEM, standard error of the mean.

monitored SG ER calcium levels within 2 hours from tape stripping. In the first 5 minutes, a 15% decrease in the FRET ratio in the SG was observed. Between 10 and 30 minutes after barrier perturbation, SG ER calcium levels increased above baseline and returned to basal levels within 2 hours after perturbation (Figure 3d). These experiments show direct evidence of ER calcium release within minutes of barrier perturbation and of subsequent actively regulated ER store refill. Moreover, these data provide a timeline for ER calcium signaling after barrier abrogation.

ER calcium release causes desmosome remodeling after barrier perturbation
ER calcium signaling has been shown to regulate cell-to-cell adhesion and desmosome adhesive strength (Aoyama et al.,
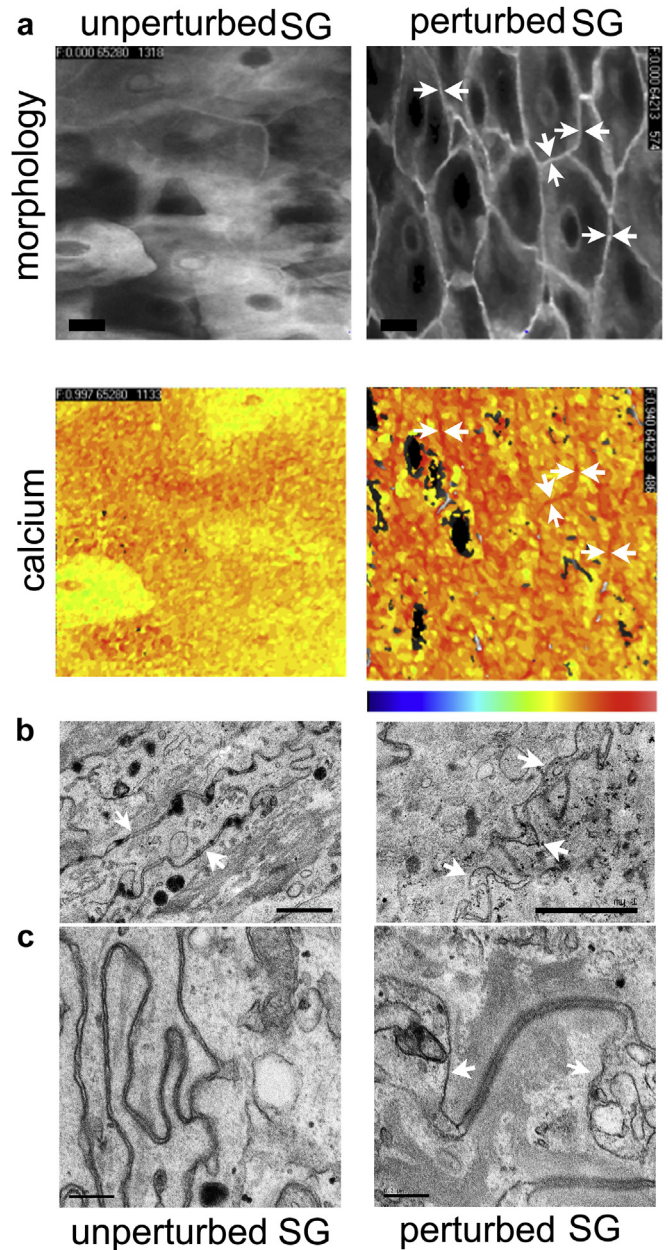

Figure 2. Morphological changes and localization of calcium pools in stratum granulosum (SG) after barrier perturbation. (a) SG cell morphology and calcium concentration distribution of calcium green 5N (CG5N) stained epidermis before and immediately after barrier perturbation as revealed by fluorescence intensity images, and false color inserts therein. Bar = 10 μm. White arrows point to extracellular calcium pools that become evident immediately after barrier perturbation. Color legend represents lowest calcium concentrations in blue (approximately 0.5 μM) and highest calcium concentration in red (approximately 50 μM). Images represent five different samples perturbed by either tape stripping or acetone lipid extraction. (b) EM micrographs of extracellular domains in the SG before and after barrier perturbation. White arrows indicate intercellular spaces between granular cells. ×4,800 magnification, bar = 1 μM. Micrographs represent four different samples per condition. (c) High-magnification electron microscopy micrographs (×19,000) showing narrow extracellular spaces in unperturbed skin samples and wide extracellular gaps (white arrows) flanking desmosomes in perturbed epidermis (left and right panel, respectively). Bar = 200 nm.

2009; Hobbs et al., 2011; Savignac et al., 2014; Stuart et al., 1996). Desmosomes are remodeled, signified by changes in the desmosomal adhesive strength and midline structures seen
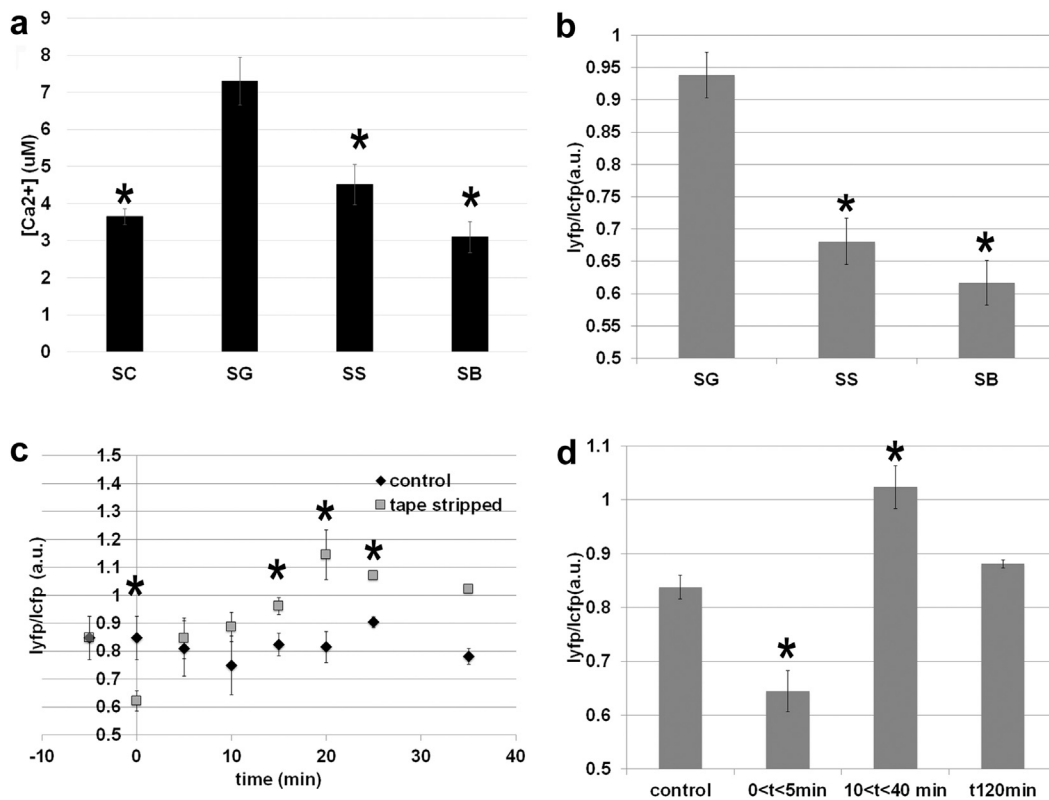
Figure 3. Intracellular and extracellular calcium fluxes in reconstructed HEEs. (**a**) Mean calcium concentration in different epidermal strata of HEEs stained with CG5N as detected by FLIM. n = 4 HEEs from two separate experiments. (**b**) Baseline ER calcium levels in different epidermal strata of D1ER transfected HEEs. (**c**) ER calcium response as a function of time in unperturbed and tape-stripped HEE SG cells transfected with D1ER as indicated by changes in the CFP-YFP FRET ratio. (**d**) ER calcium changes before and at 0 minutes $< t <$ 5 minutes, 10 minutes $< t <$ 40 minutes, $t =$ 120 minutes after barrier perturbation in the SG. N = 10–20 cells from four separate HEEs from two different experiments per condition and data point. Data are presented as mean ± SEM. Asterisks indicate statistically significant deviations from unperturbed SG calcium levels, $P < 0.02$. CFP, cyan fluorescent protein; CG5N, calcium green 5N; ER, endoplasmic reticulum; FLIM, fluorescence lifetime imaging; FRET, Förster resonance energy transfer; HEEs, human epidermal equivalents; SEM, standard error of the mean; SG, stratum granulosum; YFP, yellow fluorescent protein.

Table 1. Changes in intercellular space thickness in the lower stratum granulosum after barrier perturbation: five low-magnification (from ×4,800 to ×10,000) micrographs per condition from two independent experiments were used to measure cell-to-cell distances in the epidermal granular layer (n = 33−64 measurements per condition)

Sample	Intercellular space thickness (nm)
Untreated human skin	33 ± 7
Acetone-treated human skin	99 ± 9[1]
Tape-stripped human skin	109 ± 25[1]

[1]A statistically significant difference from the untreated sample assessed by a double-tailed *t*-test ($P < 0.02$).

on EM (Garrod and Chidgey, 2008), after processes that change epidermal or keratinocyte Ca^{2+}, such as wounding, or Darier and Hailey-Hailey disease (de Dobbeleer and Achten, 1979; Dhitavat et al., 2004; Garrod et al., 2005; Gottlieb and Lutzner, 1970; Hobbs et al., 2011; Merritt et al., 2006). Because we find marked and rapid shifts in ER and cytosolic Ca^{2+} after barrier perturbation, we next looked at cell-to-cell adhesion responses to barrier perturbation at the electron microscopy level. Although desmosome midlines were found

in unperturbed epidermis (Figure 4a), we found a statistically significant loss of the desmosomal midline immediately after barrier perturbation by either tape stripping or acetone treatment (Figure 4b and c, respectively; Table 2) in the SG and SS of human explants and HEEs. We identified desmosomes by their keratin attachments and found that in the lower SG of unperturbed human skin, 33% of desomosomes presented a distinctive dense midline that has previously been associated with a calcium-independent hyperadhesive conformation (Garrod et al., 2005). In contrast, the midline structures were found in only 9% of tape-stripped and 7% of acetone-treated samples in human skin explants (Table 2). We exposed unperturbed and tape-stripped human skin explants to calcium-free media for 1.5 hours to test the calcium dependence of the desmosomes after barrier perturbation. Although desmosomes in the unperturbed sample largely retained their structure after exposure to EGTA in agreement with Garrod et al. (2005), we did notice a diminution of the midlines that appear fainter in these samples. Exposure to EGTA of tape-stripped samples resulted in substantially altered tissue and desmosome morphology. Desmosomes were harder to identify and appeared to have lost their characteristic organization. Splitting of the two desmosomal halves was observed in some of the tissue areas, suggesting loss of hyperadhesion in these areas after barrier perturbation (Supplementary Figure S2 online).

Figure 4. **Remodeling of desmosomes in the lower stratum granulosum (SG) after barrier perturbation or endoplasmic reticulum (ER) calcium release.** (**a**) Unperturbed human epidermis; (**b**) tape-stripped human epidermis ($t = 0$); (**c**) acetone-treated human epidermis; (**d**) vehicle (1:1,000 DMSO in water) treated flank skin of a hairless mouse; (**e**) hairless mouse flank skin treated topically for 2 hours with 100 nM thapsigargin. Micrographs represent four samples from two different patients, and four samples from two mice.
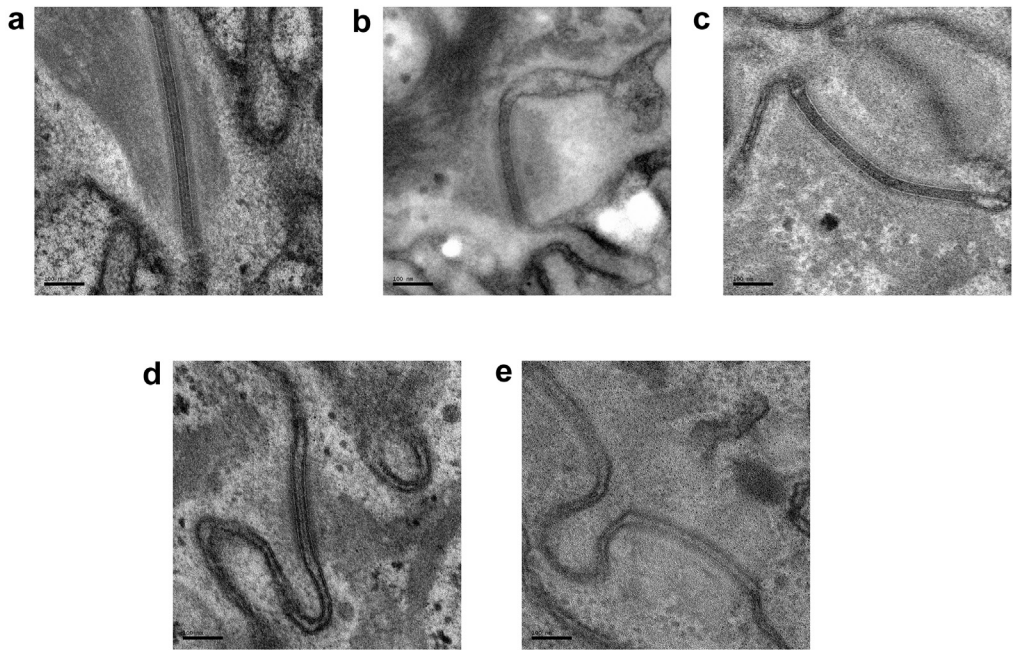
Table 2. Changes in desmosome morphology in the lower SG after barrier perturbation, and ER calcium release with thapsigargin

Sample	Total number of desmosomes	Desmosomes with midlines	Percentage midlines
Untreated human skin	63	21	33 ± 4
Acetone-treated human skin	63	4	9 ± 4[1]
Tape-stripped human skin	119	9	7 ± 2[1]
Untreated mouse skin	57	9	16 ± 5
TG-treated mouse skin	98	0	0[1]

The number of desmosomes with and without an evident midline was counted per each of 10 electron microscopy micrographs per condition from two independent experiments.
Abbreviations: ER, endoplasmic reticulum; SG, stratum granulosum; TG, thapsigargin.
[1]A statistically significant difference from the untreated control assessed by a double-tailed t-test ($P < 0.02$).

Table 3. Changes in desmosome thickness after midline loss after barrier perturbation and ER calcium release with thapsigargin

Sample	Desmosome thickness (nm)
Untreated human skin, desmosomes with midlines	25.8 ± 0.4
Acetone-treated human skin, desmosomes without midlines	22.6 ± 0.3[1]
Tape-stripped human skin, desmosomes without midlines	21.2 ± 0.5[1]
Untreated mouse skin, desmosomes with midlines	26 ± 1
TG-treated mouse skin, desmosomes without midlines	23.0 ± 0.2[2]

$N = 25-37$ desmosomes per condition from two independent experiments. Double-tailed t-tests were used to assess statistical significance.
Abbreviations: ER, endoplasmic reticulum; TG, thapsigargin.
[1]$P < 0.02$.
[2]$P < 0.05$.

Additionally, we measured the desmosomes thickness in the lower SG of unperturbed and perturbed epidermis and found that loss of the midline after both barrier perturbation and TG treatment correlates with a statistically significant thinning of the desmosomes (in agreement with Garrod et al., 2005), from an average of 25.8 ± 0.4 nm in unperturbed human epidermis, to 21.2 ± 0.5 nm in tape-stripped human epidermis (Table 3). We used HEEs to correlate ER calcium dynamics with desmosome morphology. We found that 70% of desmosomes in our mature HEEs presented midlines. Three hours after tape stripping midlines were present in only 10% of analyzed desmosomes (Figure 5b), when the ER calcium store was refilled (Figure 3c and d). The midline structure was again detected in 70% of

HEE desmosomes 24 hours after tape stripping (Figure 5c), when both the epidermal calcium gradient and epidermal permeability function were recovered (Sun et al., 2015).

To determine whether ER calcium release alone directly controls desmosomal remodeling in skin independently of barrier disruption, we treated hairless mice topically with the sarcoplasmic reticulum Ca^{2+}-ATPase isoform 2 inhibitor TG, which, as we previously demonstrated, causes ER Ca^{2+} release and sets many Ca^{2+}-dependent barrier recovery mechanisms in motion, even in the absence of barrier perturbation (Celli et al., 2011). In the lower SG of untreated mouse skin, 15% of the desmosomes identified presented a dense midline. Topical application of 100 nM TG for 2 hours resulted in the loss of the desmosomal midline in 100% desmosomes in both the SG and SS (Figure 4d and Table 2) of hairless mice epidermis.
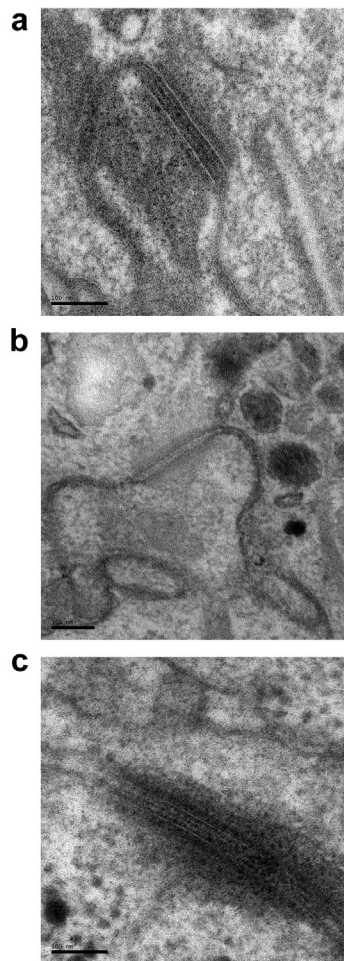
Figure 5. Reversible desmosome remodeling after barrier perturbation. (**a**) Representative desmosome morphology in the granular layer of unperturbed mature human epidermal equivalents (HEEs). (**b**) Desmosome morphology 3 hours after tape stripping HEEs. (**c**) Desmosome morphology 24 hours after tape stripping HEEs.

These experiments show that barrier perturbation alone, without wounding, causes remodeling of the desmosomal structures. Moreover, they provide evidence that ER calcium release is sufficient to cause such changes, in vivo.

DISCUSSION

With the experiments presented above, we have: (i) defined the time course for epidermal calcium signaling after barrier perturbation; (ii) demonstrated ER calcium release and re-uptake after barrier perturbation; and (iii) provided direct evidence that barrier perturbation causes desmosome remodeling consistent with loss of hyperadhesion through a mechanism controlled by ER Ca^{2+} release.

Several experimental (Celli et al., 2010; Jungman et al., 2012; Mauro et al., 1998; Menon et al., 1992; Tsutsumi et al., 2009) and computational approaches (Adams et al., 2012, 2015; Cornelissen et al., 2007; Denda et al., 2014) have been used to model or measure Ca^{2+} fluxes in epidermis. While initial studies using fixed and sectioned tissue (Mauro et al., 1998; Menon et al., 1992) showed that after acute barrier perturbation, Ca^{2+} drops in the viable layers and then recovers as the barrier recovers, a more recent study (Behne et al., 2011) reported a moderate

increase in intracellular and extracellular calcium concentration as soon as 30 minutes after barrier perturbation by acetone lipid extraction in hairless mice. We find that the conflicting results on the Ca^{2+} gradient response to barrier perturbation reported by different groups can be attributed to different experimental preparations (see Supplementary Figure S3 online).

The results presented here define the time course of epidermal calcium response to barrier perturbation. Our data are consistent with mobilization of large pools of calcium into the extracellular space within minutes after barrier perturbation.

Thanks to the subcellular resolution of the FLIM method, we are also able to resolve a dramatic increase in intracellular calcium concentration after barrier perturbation, which we showed to be due to release of ER calcium.

ER calcium signaling in keratinocytes is an important regulator of cell-to-cell adhesion. Defective ER calcium homeostasis causes desmosomal abnormalities and acantholysis in Darier disease. Recently, ER calcium signaling in keratinocytes has been linked to regulation of desmosomal adhesion through protein kinase C activation (Hobbs et al., 2011), focal adhesion turnover, cell migration, and differentiation through ORAI1-dependent store operated calcium entry (Vandenberghe et al., 2013), itch in an atopic dermatitis model through peroxisome proliferator-activated receptor 2 activation, and thymic stromal lymphopoietin release (Baek et al., 2013).

With the data presented here, we demonstrate that the epidermal permeability barrier regulates ER calcium homeostasis and release. Moreover, we show that ER calcium release in the granular layers after permeability barrier abrogation results in loss of the desmosomal midline characteristic of the hyperadhesive state of adult epidermis (Garrod and Chidgey, 2008). Garrod et al. (2005) and references within reported the loss of the desmosomal midline after wounding. Interestingly, we found that permeability barrier abrogation by acetone lipid extraction alone without tape stripping/wounding also causes desmosome remodeling and loss of the midline, thus suggesting that desmosomes respond to changes in permeability barrier function through an ER-calcium-mediated process. The experiments presented in this report provide insights into the regulation of epidermal calcium and its control of desmosome adhesiveness in live skin. Moreover, our data suggest that future computational and mathematical modeling of calcium dynamics after barrier perturbation must incorporate increased extracellular Ca^{2+} fluxes through transiently widened intercellular spaces.

MATERIALS AND METHODS
Sample preparation
Skin explants were obtained from the dermatology surgical units under protocols approved by the University of California, San Francisco, and San Francisco Veterans Affairs Medical Center and in accordance with the principles expressed in the Declaration of Helsinki. Patient consent for these explants is not necessary, as these tissues are classified as "waste," and would otherwise be discarded. Samples were tape-stripped 20–30 times using D-squames, until glistening was observed. For barrier perturbation by lipid extraction experiments, acetone was applied by gently rolling an acetone-soaked Q-tip on the skin surface for 1–2 minutes. For FLIM-based calcium measurements,

explants were incubated with a 40 µM calcium green 5N solution in cell culture media (CNT 07, CELLnTEC, Bern, Switzerland) containing 0.07 mM Ca overnight at 37 °C so that only the dermal side was in contact with the medium. After tape stripping or acetone treatment, samples to be used for the 4- and 24-hour time points were returned to the incubator in the dye-containing bathing media.

Human epidermal equivalents

Primary neonatal foreskin keratinocytes were obtained under an institutionally approved protocol. Because these tissues would otherwise be discarded, they are classified as "waste," and therefore written informed consent for this specific project was not required. Keratinocytes were isolated from neonatal foreskins and grown in 0.07 mM Ca^{2+} 154CF medium (Life Technologies) supplemented with human keratinocyte growth supplement. A suspension of second passage keratinocytes (approximately $4.42 \times 10^5/cm^2$ insert) was seeded on CELLstart CTS (Invitrogen) coated inserts (Millipore, PET, 0.4 µm) in CnT-07 (CELLnTEC) according to the manufacturer's protocol. Three days after seeding (D3), the media was switched to CnT-02-3D (CELLnTEC). On D4, the HEEs were air-exposed by feeding the bottom of the insert with CnT-02-3D. From D4 onward, HEEs were fed daily with CnT-02-3D until harvested. HEEs were grown in a dry incubator (30–50% relative humidity) at 37 °C and 5% CO_2. For FLIM-based calcium measurements, on D11, calcium green 5N was added to the growing media to a final concentration of 40 µM. On D12, cultures were washed in dye-free media to remove excess dye, removed from their insert, and secured SC down on a microscope cover glass. For barrier perturbation and recovery after tape stripping, a precut D-squame (CuDerm, D100) was applied on top of HEE and was carefully stripped away from HEE. Cultures were then returned to 37 °C, 5% CO_2, 30% humidity. Control HEEs were not tape-stripped. Cultures were excised from their inserts and placed SC down on a cover glass and mounted on the microscope for calcium flux visualization.

ER Ca^{2+} sequestration

Cells were transfected with the ER-targeted cameleon-based Ca^{2+} sensor D1ER (gift of Dr Amy Palmer; Palmer et al., 2006) using the lipid-based Trans-it transfection reagent (Mirus) at a 1:3 DNA:Trans-it ratio. Transfection complexes were assembled 30 minutes before cell plating by adding 1 µl D1ER (at a 1.3 µg/µl concentration) and 3 µl transfection reagent per 100 µl serum-free OptiMem. Cells were resuspended in low calcium 154CF medium supplemented with 0.03 mM Ca^{2+} (Gibco) at a density of 0.5×10^6 cells per 1.5 ml. Transfection complexes were added to the suspension in a 100 µl:1 ml complexes to cell suspension ratio and gently mixed by pipetting. Cells were then plated into 12-well inserts precoated with CELLstart at a 0.5×10^6 cells per insert density and left with the transfection complexes overnight. The media was then switched to CnT.BM.1 medium with CnT-07 supplement (CELLnTEC) for 3 days after which cultures were fed regularly, as described above. Dual-channel fluorescence measurements were recorded using a Zeiss LSM Meta confocal system (Zeiss) as described in Celli et al. (2011). Briefly, two-photon excitation at 800 nm was used to excite the CFP moiety of D1ER. CFP and YFP fluorescence were detected using a NFT 490 dichroic mirror and 450/35 and 550/35 band-pass filters. The $I_{(YFP)}/I_{(CFP)}$ intensity ratio was calculated after background subtraction using Matlab (The MathWorks, Natick, MA).

Thapsigargin mouse treatment

Mice were treated under protocols approved by the University of California, San Francisco, and San Francisco Veterans Affairs Medical Center. Normal hairless mice were anesthetized with 40 mg/ml chloral hydrate and received dorsal flank treatments with a vehicle of 70% propylene glycol and 30% ethanol mixture or 100 nM TG in the vehicle. Two hours later, mice were euthanized and skin biopsies were harvested. Samples for electron microscopy were placed immediately in modified Karnovsky's fixative, according to a previous protocol (Elias et al., 2002b).

Transmitted electron microscopy

The samples were processed as previously described (Ilic et al., 2007; Tu et al., 2012). Briefly, the HEEs were fixed in modified Karnovsky's fixative (2% formaldehyde and 2% glutaraldehyde in 0.1 M cacodylate buffer, pH 7.2) and post-fixed in either 0.2% RuO_4 or 1% OsO_4. For ion-capture cytochemistry, the HEE samples were fixed in ice-cold fixative containing 2% glutaraldehyde, 2% formaldehyde, 90 mM potassium oxalate, and 1.4% sucrose (pH 7.4) in the dark for 1–2 hours. The samples were then post-fixed in 1% OsO_4 containing 2% potassium pyroantimonate at 4 °C in the dark for 2 hours. All samples were then dehydrated and embedded in Spurr's resin. Ultrathin sections stained with uranyl acetate and lead citrate were examined in a Zeiss 10CR transmission electron microscope (Zeiss). Desmosomes were identified by their keratin attachments at a ×10,000 magnification. For each sample and condition, we acquired 10 fields of view sampling both the SG and SS. For each field of view, we counted the total number of desmosomes and desmosomes presenting midlines, and calculated their ratio. Data are presented as mean values ± SEM.

FLIM imaging and data analysis

FLIM z-stacks of human ex vivo and in vitro epidermis stained with calcium green 5N were acquired, as previously described in Celli et al. (2010). In brief, samples were placed SC down on a cover glass and mounted on an inverted Zeiss LSM NLO 510 microscope (Zeiss, NY), connected to a photon counting TCSPC card (Becker and Hickle, Germany). A mode-locked Ti:sapphire laser (Mira 900, Coherent, CA) tuned at 800 nm was used as a source of multiphoton excitation. FLIM data were referenced against a fluorescein standard solution (1 mM in Tris buffer at pH 10) and analyzed using the phasor approach (Celli et al., 2010) with the software SimFCS (Laboratory for Fluorescence Dynamics, UCI, Irvine, CA). Calcium concentration histograms were calculated for each FLIM image, and the calcium concentration corresponding to the distribution peak was recorded. Data are presented as the averaged position of the calcium concentration peak in each epidermal layer ± SEM ($5 < n < 10$ per layer per condition from 2 to 5 independent experiments).

Statistical analysis

Statistically significant differences among populations were determined by performing one-way ANOVA and two-tailed *t*-tests.

CONFLICT OF INTEREST
The authors state no conflict of interest.

SUPPLEMENTARY MATERIAL

Supplementary material is linked to the online version of the paper at www.jidonline.org, and at http://dx.doi.org/10.1016/j.jid.2016.05.100.

REFERENCES

Adams MP, Mallet DG, Pettet GJ. Active regulation of the epidermal calcium profile. J Theor Biol 2012;301:112−21.

Adams MP, Mallet DG, Pettet GJ. Towards a quantitative theory of epidermal calcium profile formation in unwounded skin. PLoS One 2015;10: e0116751.

Aoyama Y, Yamamoto Y, Yamaguchi F, Kitajima Y. Low to high Ca^{2+}-switch causes phosphorylation and association of desmocollin 3 with plakoglobin and desmoglein 3 in cultured keratinocytes. Exp Dermatol 2009;18:404−8.

Baek JH, Lee SE, Choi KJ, Choi EH, Lee SH. Acute modulations in stratum corneum permeability barrier function affect claudin expression and epidermal tight junction function via changes of epidermal calcium gradient. Yonsei Med J 2013;54:523−8.

Behne MJ, Sanchez S, Barry NP, Kirschner N, Meyer W, Mauro TM, et al. Major translocation of calcium upon epidermal barrier insult: imaging and quantification via FLIM/Fourier vector analysis. Arch Dermatol Res 2011;303:103−15.

Celli A, Mackenzie DS, Crumrine DS, Tu CL, Hupe M, Bikle DD, et al. Endoplasmic reticulum Ca(2+) depletion activates XBP1 and controls terminal differentiation in keratinocytes and epidermis. Br J Dermatol 2011;164:16−25.

Celli A, Mackenzie DS, Zhai Y, Tu CL, Bikle DD, Holleran WM, et al. SERCA2-controlled Ca(2)+-dependent keratinocyte adhesion and differentiation is mediated via the sphingolipid pathway: a therapeutic target for Darier's disease. J Invest Dermatol 2012;132:1188−95.

Celli A, Sanchez S, Behne M, Hazlett T, Gratton E, Mauro T. The epidermal Ca(2+) gradient: measurement using the phasor representation of fluorescent lifetime imaging. Biophys J 2010;98:911−21.

Cornelissen LH, Oomens CW, Huyghe JM, Baaijens FP. Mechanisms that play a role in the maintenance of the calcium gradient in the epidermis. Skin Res Technol 2007;13:369−76.

de Dobbeleer G, Achten G. Disrupted desmosomes in induced lesions of familial benign chronic pemphigus. J Cutan Pathol 1979;6:418−24.

Denda M, Denda S, Tsutsumi M, Goto M, Kumamoto J, Nakatani M, et al. Frontiers in epidermal barrier homeostasis—an approach to mathematical modelling of epidermal calcium dynamics. Exp Dermatol 2014;23:79−82.

Denda S, Kumamoto J, Takei K, Tsutsumi M, Aoki H, Denda M. Ryanodine receptors are expressed in epidermal keratinocytes and associated with keratinocyte differentiation and epidermal permeability barrier homeostasis. J Invest Dermatol 2012;132:69−75.

Dhitavat J, Fairclough RJ, Hovnanian A, Burge SM. Calcium pumps and keratinocytes: lessons from Darier's disease and Hailey-Hailey disease. Br J Dermatol 2004;150:821−8.

Elias PM, Ahn S, Brown B, Crumrine D, Feingold KR. Origin of the epidermal calcium gradient: regulation by barrier status and role of active vs passive mechanisms. J Invest Dermatol 2002a;119:1269−74.

Elias PM, Ahn SK, Denda M, Brown BE, Crumrine D, Kimutai LK, et al. Modulations in epidermal calcium regulate the expression of differentiation-specific markers. J Invest Dermatol 2002b;119:1128−36.

Feingold KR, Denda M. Regulation of permeability barrier homeostasis. Clin Dermatol 2012;30:263−8.

Garrod D, Chidgey M. Desmosome structure, composition and function. Biochim Biophys Acta 2008;1778:572−87.

Garrod DR, Berika MY, Bardsley WF, Holmes D, Tabernero L. Hyper-adhesion in desmosomes: its regulation in wound healing and possible relationship to cadherin crystal structure. J Cell Sci 2005;118:5743−54.

Gottlieb SK, Lutzner MA. Hailey-hailey disease—an electron microcopic study. J Invest Dermatol 1970;54:368−76.

Hobbs RP, Amargo EV, Somasundaram A, Simpson CL, Prakriya M, Denning MF, et al. The calcium ATPase SERCA2 regulates desmoplakin

dynamics and intercellular adhesive strength through modulation of PKCα signaling. FASEB J 2011;25:990−1001.

Hu Z, Bonifas JM, Beech J, Bench G, Shigihara T, Ogawa H, et al. Mutations in ATP2C1, encoding a calcium pump, cause Hailey-Hailey disease. Nat Genet 2000;24:61−5.

Ilic D, Mao-Qiang M, Crumrine D, Dolganov G, Larocque N, Xu P, et al. Focal adhesion kinase controls pH-dependent epidermal barrier homeostasis by regulating actin-directed Na^+/H^+ exchanger 1 plasma membrane localization. Am J Pathol 2007;170:2055−67.

Jungman E, Pirot F, Maibach H. Ex vivo calcium percutaneous eggression in normal and tape-stripped human skin. Cutan Ocul Toxicol 2012;31:1−6.

Man MQ, Mauro T, Bench G, Warren R, Elias PM, Feingold KR. Calcium and potassium inhibit barrier recovery after disruption, independent of the type of insult in hairless mice. Exp Dermatol 1997;6:36−40.

Mauro T, Bench G, Sidderas-Haddad E, Feingold K, Elias P, Cullander C. Acute barrier perturbation abolishes the Ca^{2+} and K^+ gradients in murine epidermis: quantitative measurement using PIXE. J Invest Dermatol 1998;111:1198−201.

Menon GK, Elias PM. Ultrastructural localization of calcium in psoriatic and normal human epidermis. Arch Dermatol 1991;127:57−63.

Menon GK, Elias PM, Feingold KR. Integrity of the permeability barrier is crucial for maintenance of the epidermal calcium gradient. Br J Dermatol 1994;130:139−47.

Menon GK, Elias PM, Lee SH, Feingold KR. Localization of calcium in murine epidermis following disruption and repair of the permeability barrier. Cell Tissue Res 1992;270:503−12.

Merritt AJ, Scothern A, Bhattacharyya T. Assays for the calcium sensitivity of desmosomes. Methods Mol Biol 2006;341:167−83.

Palmer AE, Giacomello M, Kortemme T, Hires SA, Lev-Ram V, Baker D, et al. Ca^{2+} indicators based on computationally redesigned calmodulin-peptide pairs. Chem Biol 2006;13:521−30.

Petrova A, Celli A, Jacquet L, Dafou D, Crumrine D, Hupe M, et al. 3D In vitro model of a functional epidermal permeability barrier from human embryonic stem cells and induced pluripotent stem cells. Stem Cell Reports 2014;2:675−89.

Savignac M, Simon M, Edir A, Guibbal L, Hovnanian A. SERCA2 dysfunction in Darier disease causes endoplasmic reticulum stress and impaired cell-to-cell adhesion strength: rescue by Miglustat. J Invest Dermatol 2014;134: 1961−70.

Stuart RO, Sun A, Bush KT, Nigam SK. Dependence of epithelial intercellular junction biogenesis on thapsigargin-sensitive intracellular calcium stores. J Biol Chem 1996;271:13636−41.

Sun R, Celli A, Crumrine D, Hupe M, Adame LC, Pennypacker SD, et al. Lowered humidity produces human epidermal equivalents with enhanced barrier properties. Tissue Eng Part C Methods 2015;21:15−22.

Tariq H, Bella J, Jowitt TA, Holmes DF, Rouhi M, Nie Z, et al. Cadherin flexibility provides a key difference between desmosomes and adherens junctions. Proc Natl Acad Sci USA 2015;112:5395−400.

Thomason HA, Cooper NH, Ansell DM, Chiu M, Merrit AJ, Hardman MJ, et al. Direct evidence that PKCalpha positively regulates wound re-epithelialization: correlation with changes in desmosomal adhesiveness. J Pathol 2012;227:346−56.

Trollinger DR, Isseroff RR, Nuccitelli R. Calcium channel blockers inhibit galvanotaxis in human keratinocytes. J Cell Physiol 2002;193:1−9.

Tsutsumi M, Denda S, Inoue K, Ikeyama K, Denda M. Calcium ion gradients and dynamics in cultured skin slices of rat hindpaw in response to stimulation with ATP. J Invest Dermatol 2009;129:584−9.

Tu CL, Crumrine DA, Man MQ, Chang W, Elalieh H, You M, et al. Ablation of the calcium-sensing receptor in keratinocytes impairs epidermal differentiation and barrier function. J Invest Dermatol 2012;132:2350−9.

Vandenberghe M, Raphael M, Lehen'kyi V, Gordienko D, Hastie R, Oddos T, et al. ORAI1 calcium channel orchestrates skin homeostasis. Proc Natl Acad Sci USA 2013;110:E4839−48.

Wallis S, Lloyd S, Wise I, Ireland G, Fleming TP, Garrod D. The alpha isoform of protein kinase C is involved in signaling the response of desmosomes to wounding in cultured epithelial cells. Mol Biol Cell 2000;11:1077−92.

Yuspa SH, Kilkenny AE, Steinert PM, Roop DR. Expression of murine epidermal differentiation markers is tightly regulated by restricted extracellular calcium concentrations in vitro. J Cell Biol 1989;109:1207−17.